Structure of Isolated Tryptophyl-Glycine Dipeptide and Tryptophyl-Glycyl-Glycine Tripeptide: Ab Initio SCC-DFTB-D Molecular Dynamics Simulations and High-Level Correlated ab Initio Quantum Chemical Calculations

Haydee Valdés, David Řeha, and Pavel Hobza*

Institute of Organic Chemistry and Biochemistry, Academy of Sciences of the Czech Republic, and Center for Biomolecules and Complex Molecular Systems, 166 10 Prague 6, Czech Republic

Received: December 21, 2005; In Final Form: January 25, 2006

The tryptophyl-glycine (Trp-Gly) and tryptophyl-glycyl-glycine (Trp-Gly-Gly) peptides have been studied by means of molecular dynamic simulations combined with high-level correlated ab initio quantum chemical and statistical thermodynamic calculations. The lowest energy conformers were localized in the free energy surface. The structures of the different Trp-Gly and Trp-Gly-Gly conformers coexisting in the gas phase have been for the first time reported and their scaled theoretical IR spectra unambiguously assigned and compared with previous gas-phase experimental results. Common geometrical features have been systematically observed for the sequence Trp, Trp-Gly, and Trp-Gly-Gly. In addition, the peptide backbone of Trp-Gly-Gly has been compared with that of the previously studied Phe-Gly-Gly (Reha, D. et. al. *Chem. Eur. J.* **2005**, *11*, 6803). From the observed systematic structural behavior between these peptide analogues, it is expected that the gas-phase conformers of other similar aromatic small peptides would present equivalent geometries. The DFT methodology failed to describe the potential energy surface of the studied peptides since the London dispersion energy (not covered in DFT) plays a significant role in the stabilization of most stable conformers.

Introduction

The study of peptide chains in the gas phase is of great importance as the information obtained can be helpful understanding the protein-folding process. Gas-phase studies allow us to obtain the intrinsic (without influence of the environment) properties of isolated peptides. They also provide very useful information concerning the interactions responsible for the structural motifs in the peptide chain which can play a key role in the initiation phase of the folding process. Finally, they constitute the unique approach for describing the folding processes in a hydrophobic medium, such as the protein interior or lipidic membranes.

The study of isolated peptides containing aromatic rings is of special importance as these systems absorb in the UV spectral region. UV double-resonance spectroscopy techniques allow for a selection of distinct isomers, and therefore, properties of isolated conformers can be obtained. However, small peptides are thought to be generally nonrigid (floppy) molecules, and obtaining high resolved spectra is complicated. Thus, theoretical studies are needed to support the assignments of spectral data and for visualization of molecular processes. Recently, it has been shown[1] that the combination of the ab initio self-consistent-charge density functional tight-binding method with the inclusion of an empirical term for describing the dispersion energy (SCC-DFTB-D) molecular dynamics/quenching (MD/Q) procedure with high-level correlated ab initio quantum chemical calculations is an efficient tool for the study of amino acids and small peptide systems. By means of this accurate theoretical treatment, it is possible to obtain the most stable conformers on the free energy surface (FES) as well as their relative abundances at thermodynamic equilibrium conditions. Further, based on the direct comparison of the calculated molecular properties (for example, vibrational frequencies) with the experimental ones, the structure found by the experiment can be easily assigned. It was also shown[1] that the standard density functional theory (DFT) methodology fails because several peptide conformers (and even the global minimum) are stabilized by long-range London dispersion forces not considered in DFT. Unlike the DFT studies commonly performed for small peptides, the presently used procedure provides a proper description of the dispersion forces and, thus, gives a complete conformational landscape. Moreover, it overcomes some of the deficiencies of the frequently used empirical force fields, namely, a bad description (or sometimes absence) of the polarization, the conformational dependence of the atomic charges, and the absence of charge-transfer effects.[2]

There are four aromatic amino acids which can be found in proteins, namely, phenylalanine (Phe), tyrosine (Tyr), tryptophan (Trp), and histidine (His). The structure and infrared spectrum of some of them, as well as their sequentially related peptides, have been published already,[1−8] but so far, the conformations of tryptophyl-glycine (Trp-Gly) and tryptophyl-glycyl-glycine (Trp-Gly-Gly) peptides are yet unknown. Trp-Gly dipeptide and Trp-Gly-Gly tripeptide have been studied for the first time by means of UV spectroscopic methods by Levy and co-workers.[9] The broad absorption bands observed in their recorded spectra suggested the possible existence of several conformers. However, no structural analysis was reported on these systems. Recently, Kleinermanns et al.[10,11] investigated these peptides by means of UV−UV and IR−UV hole-burning spectroscopy. From these experiments combined with DFT calculations, the authors were not able to assign unambiguously the different spectra to different conformers, and no conclusive information concerning the geometry of the peptides was provided.

* To whom correspondence should be addressed at the Institute of Organic Chemistry and Biochemistry. Fax: +420-220 410 320. E-mail: pavel.hobza@uochb.cas.cz.

10.1021/jp057425y CCC: $33.50
Published on Web 03/07/2006

CHART 1: Strategy of Calculation for Selecting the Most Stable and Populated Conformers

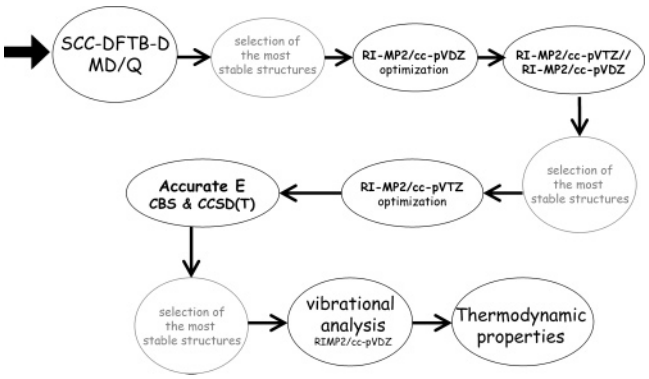

Here, we present a high-level theoretical study on Trp-Gly and Trp-Gly-Gly peptides by means of the combination of ab initio SCC-DFTB-D MD/Q simulations and high-level correlated ab initio quantum chemical calculations. Our calculated vibrational spectra match the experimental spectra better than the previously suggested structures[10,11] and allow for a clear assignment of the conformers. The geometries of the Trp-Gly dipeptide and Trp-Gly-Gly tripeptide will be compared with that of the Trp amino acid.[4] By this systematic structural study of Trp-related peptides it will be possible to elucidate their structural features relationship.

2. Methodology

2.1. Strategy of Calculation. According to the theoretical procedure previously employed for the study of Phe-Gly-Gly[1] tripeptide (see Chart 1), we have performed the first screening of the potential energy surface (PES) of Trp-Gly and Trp-Gly-Gly peptides by means of ab initio SCC-DFTB-D MD/Q simulations. The lowest energy minima in the PES (within an energy interval of ~4 kcal/mol) were then reoptimized at the RI-MP2/cc-pVDZ level of theory and their energies further recalculated at the RI-MP2/cc-pVTZ//RI-MP2/cc-pVDZ level of theory. Then, the most stable conformers of this set (within an energy interval of ~2 kcal/mol for Trp-Gly and ~3.5 kcal/mol for Trp-Gly-Gly) were fully reoptimized at the RI-MP2/cc-pVTZ level of theory. For this final set of structures, we determined accurate total energies (sum of complete basis set (CBS) limit of the MP2 energy and the CCSD(T) correction term) as well as harmonic vibrational frequencies (RI-MP2/cc-pVDZ).

Harmonic vibrational frequencies were calculated using a numerical Hessian. The frequencies obtained were scaled with different scaling factors depending on the type of vibration mode. The factors 0.956, 0.951, and 0.958 were used for the OH stretch, for the NH stretch of the peptide bond, and for the NH stretch of the indole ring, respectively. Finally, the factor 0.956 (median) was used as an universal factor for the remaining vibrational modes. All of the scaling factors were obtained as a ratio between the theoretical and experimental frequencies for the Trp-Gly, Trp-Gly-Gly, and Phe-Gly-Gly[1] set of assigned structures using the least squares fitting method. We have shown recently[12] that scaled harmonic frequencies of the guanine-cytosine WC base pair agree better with the experimental frequencies than the anharmonic ones (VSCF treatment). This is especially true if different scaling factors are used for different frequencies. Since the gas-phase experiments are not performed at temperatures close to 0 K, it is necessary to pass from the PES to the FES. To calculate enthalpies, we have determined the zero-point vibrational energies (ZPE) from the calculated harmonic vibrational frequencies. All of the thermodynamic properties (entropy and free Gibbs energies) were calculated under the assumption of the rigid rotor−harmonic oscillator−ideal gas (RR−HO−IG) approximation. Thermodynamic characteristics determined in this way are based on the MP2/cc-pVDZ ab initio molecular constants (optimal geometry and complete set of normal vibration modes scaled by the universal scaling factor 0.956).

2.2. Computational Methods. *Molecular Dynamics/Quenching (MD/Q) Calculations.* MD/Q calculations were performed using the approximate self-consistent-charge, density functional tight-binding method with the inclusion of an empirical term for describing the dispersion energy.[13,14] An initial distribution of velocities was calculated according to a temperature of 900 K. The basic procedure of quenching consists of interrupting the MD simulation repeatedly after a limited number of steps, removing the kinetic energy term, and then performing a nonrestricted minimization using the conjugate gradient method. The energies and coordinates of the resulting minima are stored, and subsequently, the MD simulation continues from the point where it was stopped.[15] After performing the MD/Q run, all the conformers are sorted on the basis of their energies as well as on the basis of their geometries. This procedure reduces the initial set of energy minimized structures to a set of geometrically distinct structures, which correspond to all the existing minima in the PES.

High-Level Correlated ab Initio Quantum Chemical Calculations. All geometry optimizations were carried out at the RI-MP2/cc-pVXZ (X = D, T) level of theory.[16−20] Single-point calculations were performed at RI-MP2/cc-pVQZ//RI-MP2/cc-pVTZ and RI-MP2/cc-pVTZ//RI-MP2/cc-pVDZ levels of theory. Total energies were extrapolated to the complete basis set (CBS) limit using the extrapolation scheme of Helgaker and coworkers[21]

$$E_X^{HF} = E^{HF}_{CBS} + A\exp(-\alpha X) \text{ and } E_X^{corr} = E^{corr}_{CBS} + BX^{-3} \quad (1a,1b)$$

where E_X and E_{CBS} are energies for the basis set with the largest angular momentum X and for the complete basis set respectively, and A, B, and α are parameters (α = 1.43 and 1.54 for T → Q extrapolations were taken from the literature,[21] whereas A and B were fitted).

CBS CCSD(T) relative energies were calculated as follows

$$E^{CCSD(T)}_{CBS} = E^{MP2}_{CBS} + (E^{CCSD(T)} - E^{MP2})|_{\text{small basis set}} \quad (2)$$

where the first term represents the CBS limit of the relative MP2 energy obtained as a sum of eqs 1a and 1b and the second term describes the higher-order contributions to the correlation energy (beyond the second perturbation order). This difference is known to be essentially independent of the basis set size (contrary to the MP2 and CCSD(T) energies themselves).[22] It has been shown[23] that the 6-31G*(0.25) basis set provides satisfactory values of the CCSD(T)-MP2 difference for molecular clusters, and thus, we have used it systematically for all of the present CCSD(T) calculations.

Density Functional Theory Calculations. Density functional theory (DFT) calculations are currently widely used for predicting structures and energies of isolated systems as well as of molecular clusters. Specifically, many experimental studies of small peptides in the gas phase are usually combined with DFT calculations performed on the a priori most likely conformers. The high CPU performance of the DFT method allows the study

CHART 2: Torsional Angles of the Trp-Gly Dipeptide and Trp-Gly-Gly Tripeptide

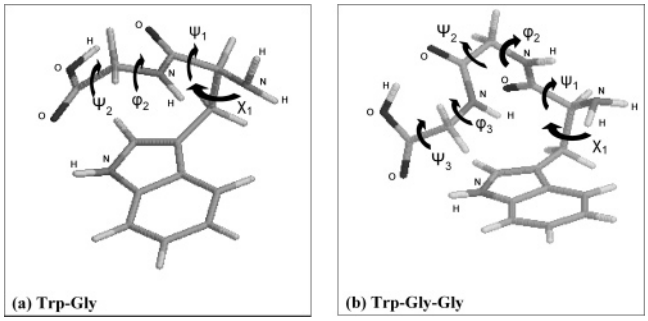

of such types of systems at a low computational cost and at an accuracy comparable to the one obtained using the correlated ab initio methods. However, one notorious drawback of the DFT methodology is its inability to properly describe the London dispersion energy. Previous studies have shown[1,24] that the DFT method fails for the description of those structures where the dispersion interaction plays an important role (i.e., stacked DNA base pairs, peptide backbone−aromatic side chain interactions). For the present paper, we have used the resolution of identity[16] (RI) approach to perform the DFT calculations. The TPSS functional[25] has been chosen as it gives comparable results with the B3LYP hybrid functional.[26] All of the calculations were performed with the cc-pVTZ basis set.[19,20]

Nomenclature of the Structures. The nomenclature used describes both the order of the conformers according to their enthalpies (H_0) and their peptide backbone geometry described in terms of its principal torsional angles (see Chart 2). The pattern followed for the peptides names is wgNN[χ_1.ψ_1.φ_2] and wggNN[χ_1.ψ_1.φ_2.ψ_2.φ_3] for the Trp-Gly and Trp-Gly-Gly, respectively. NN stands for the energetic position of the conformer according to the enthalpy scale. χ_1, ψ_1, φ_2, ψ_2, and φ_3 are the principal torsional angles (see Chart 2). Their possible values (in degrees) are the following: (a) $\chi_1 = 60$ (g+), −60 (g−), or 180 (t); (b) $\psi_1 = -20$, 0, 20, or 140; (c) $\varphi_2 = -140$, −100, −70, 70, 110, 140; (d) $\psi_2 = -10$, −60, 0, 60, 110, and finally, (e) $\varphi_3 = -70$, 70. A shortcut has been used for the name of the structures along the text.

Codes. Energies, geometries, harmonic vibrational frequencies and thermodynamic characteristics (RI-MP2 and RI-DFT) were determined using TURBOMOLE 5.7 program package.[27] CCSD(T) calculations were done with the MOLPRO 2002.6 program.[28] NBO analysis was done using GAUSSIAN 03 package.[29] MD/Q simulations were performed using SCC-DFTB-D[13,14] code and finally, the selection of the geometrically distinct structures was done using our own scripts.

3. Results and Discussion

Trp-Gly. Table 1 shows the relative RI-MP2/cc-pVTZ and RI-MP2/cc-pVQZ//RI-MP2/cc-pVTZ energies as well as the extrapolated CBS RI-MP2 relative energies for the 15 most stable minima localized in the PES of Trp-Gly by means of the SCC-DFTB-D MD/Q technique. The fifth and sixth column of Table 1 contain the CCSD(T) correction terms and the final relative CBS CCSD(T) energies, respectively, while the last column give relative values of total enthalpies (considered here as the benchmark data).

The CCSD(T) correction term ranges from −0.23 to 1.56 kcal/mol, which means that its omission can cause an error in relative energies of about 1.8 kcal/mol. Notice that for the Trp-Gly case, the inclusion of this correction term is essential for the assignment of the global minimum as at the lower levels of theory (columns 2−4) more than one conformer happen to have the same relative energy. The order of the structures changes when passing from the RI-MP2/cc-pVTZ level of theory (column 2) to the CCSD(T)/CBS level (column 6). The order of structures from the former procedure was wg02 = wg03 < wg01 < wg08 < wg09 < wg06 with an energy interval of 0.86 kcal/mol while the order of structures of the latter procedure is wg01 < wg02 < wg03 < wg05 < wg04 < wg06 with a broader energy interval of 1.32 kcal/mol. The CCSD(T)/CBS procedure substantially increases the relative energies and now the 15 structures presented in Table 1 lie within an interval of ∼3 kcal/mol. The inclusion of the ZPE does not practically affect the relative energies. From the last column of Table 1 it is evident that 10 structures lie within 2.0 kcal/mol of relative enthalpy limit, and this set will be considered for the subsequent calculation of the thermodynamic properties (see Table 2).

Figure 1 shows the RI-MP2/cc-pVTZ geometries for the 15 most stable conformers in the PES of Trp-Gly dipeptide. For all of the conformers collected in Figure 1, the peptide bond (O=C−N−H) is in a *trans* conformation. Notice that the first conformer localized in the PES with the peptide bond in a *cis* conformation is about 6 kcal/mol higher in energy (at the RI-MP2/cc-pVTZ//RI-MP2/cc-pVDZ level of theory) than the global minimum. The different conformers of the Trp-Gly dipeptide are described by eight torsional angles from which we will only discuss the four shown in Chart 2a.

First, the χ_1 torsional angle determines the rotameric state of the side chain. In case of the 15 most stable conformers of Trp-Gly, the *g*+ rotameric state ($\chi_1 \sim +60°$) is clearly preferred as only four out of the fifteen conformers have a trans rotameric state ($\chi_1 \sim 180°$) and no conformer is in a g− rotameric state ($\chi_1 \sim -60°$). The first conformer with g− rotameric state is ∼5 kcal/mol less stable (RIMP2/cc-pVTZ) than the global minimum conformation.

The ψ_1 torsional angle can be −20° (for the majority of the conformers), 140°, or 0°. In the first two cases, the $NH_{pep}\cdots\pi$ interaction is favored (i.e., wg08), whereas in the second case, the $NH_{pep}\cdots N(H_2)$ interaction is preferred (i.e., wg01). Interestingly, these latter conformers also benefit from an additional $NH_2\cdots\pi$ interaction, and thus, they are stabilized by a $NH_{pep}\cdots N(H_2)\cdots\pi$ cooperative hydrogen bonded "daisy chain" interaction.[4] This hydrogen bond cooperativity has been already observed in some other amino acids.[3,4]

Finally, φ_2 and ψ_2 torsional angles determine the position of the carboxyl group and therefore, the possible formation of a $OH_{carb}\cdots O{=}C_{pep}$ intramolecular H-bond. The existence of such H-bond means it is possible to distinguish between two families of conformers: those with a more bent (via a $OH_{carb}\cdots O{=}C_{pep}$ intramolecular H-bond) peptide backbone (i.e., wg01) and those with a quite stretched (less bent; without a $OH_{carb}\cdots O{=}C_{pep}$ intramolecular H-bond) peptide backbone (i.e., wg07). Also interesting is that the usually preferred *syn* conformation of the carboxyl group (O=C−O−H = 0°) is lost when the $OH_{carb}\cdots O{=}C_{pep}$ intramolecular H-bond is formed, and instead, an *anti* configuration (O=C−O−H = 180°) is adopted (see wg01 vs wg07). Apparently, this usually preferred *syn* configuration of the carboxyl group is sacrificed in favor of the stability gained from the intramolecular H-bonds formed.

The global minimum conformation (wg01) is stabilized by three intramolecular H-bonds, namely: $OH_{carb}\cdots O{=}C_{pep}$, $NH_{pep}\cdots N(H_2)$ and $NH_2\cdots\pi$. According to the natural bond orbital (NBO) analysis performed using the B3LYP electron densities,[30] the second-order perturbation energies for these

TABLE 1: Relative Energies and Relative Enthalpies at 0 K (in kcal/mol) for the Most Stable Conformers of Trp-Gly Dipeptide Evaluated with Various Basis Sets (Structures Are Labeled According to Figure 1)

structure	RI-MP2/cc-pVTZ	RI-MP2/cc-pVQZ	T → Q[a]	MP2 → CCSD(T)[b]	*E*[c]	*H*[d]
wg01[g+.0.70]	0.00	0.00	0.00	0.00	0.00	0.00
wg02[t.140.−70]	−0.11	−0.05	0.00	0.42	0.42	0.44
wg03[g+.−20.70]	−0.11	0.26	0.53	0.50	1.03	1.01
wg04[g+.0.−70]	1.82	1.62	1.47	−0.23	1.24	1.18
wg05[g+.0.−70]	1.48	1.26	1.10	0.13	1.23	1.20
wg06[t.140.−70]	0.86	0.89	0.92	0.40	1.32	1.29
wg07[t.140.−140]	1.19	1.14	1.10	1.17	2.27	1.60
wg08[g+.−20.140]	0.59	0.70	0.78	1.56	2.34	1.63
wg09[g+.0.110]	0.81	0.72	0.66	1.49	2.15	1.65
wg10[g+.0.70]	1.55	1.45	1.37	1.03	2.40	1.97
wg11[g+.−20.−70]	1.79	1.71	1.65	0.61	2.26	2.10
wg12[t.140.−140]	1.83	1.70	1.60	1.24	2.84	2.14
wg13[g+.−20.140]	1.15	1.16	1.17	1.54	2.71	2.24
wg14[g+.−20.70]	1.74	1.88	1.98	0.46	2.43	2.46
wg15[g+.−20.110]	1.18	1.52	1.77	1.27	3.04	2.72

[a] Extrapolation to the CBS limit using cc-pVTZ and cc-pVQZ energies. [b] Difference between CCSD(T) and MP2 relative energies determined with the 6-31g*(0.25) basis set. [c] Total relative energy evaluated as a sum of CBS RI-MP2 relative energy and a difference between CCSD(T) and MP2 relative energies. [d] ZPE were calculated at the RIMP2/cc-pVDZ level of theory.

TABLE 2: Relative Free Gibbs Energies (*G*) and Corresponding Relative Populations Calculated at $T = 300$ K According to the Maxwell−Boltzmann Distribution (MBD) Equation for the 10 Most Stable Conformers of Trp-Gly Dipeptide

structure	*G* (kcal/mol)	MBD
wg01[g+.0.70]	0.00	1000
wg08[g+.−20.140]	0.21	698
wg02[t.140.−70]	0.94	207
wg07[t.140.−140]	1.05	172
wg03[g+.−20.70]	1.09	159
wg09[g+.0.110]	1.13	151
wg05[g+.0.−70]	1.63	65
wg10[g+.0.70]	1.72	56
wg06[t.140.−70]	1.89	42
wg04[g+.0.−70]	3.06	6

interactions are 18.2, 6.2, and 1.7 kcal/mol, respectively. This allows us to classify these three intramolecular bonds as strong ($OH_{carb}\cdots O{=}C_{pep}$), medium ($NH_{pep}\cdots N(H_2)$), and weak ($NH_2\cdots\pi$). Apparently, the Trp in the global minimum conformation of Trp-Gly nicely resembles the global minimum conformation the of tryptophan amino acid[4] (see Chart 3a). Besides, the global minimum conformation of Trp-Gly dipeptide is also analogous to the global minimum conformation obtained by means of Monte Carlo replica-exchange calculations on the gas-phase Trp-Gly dipeptide in a static electric field.[31]

Kleinermanns and co-workers[10,11] have recently performed resonant two-photon ionization (REMPI) and UV−UV and IR−UV hole-burning experiments on Trp-Gly dipeptide. In these experiments, the peptides were evaporated by laser desorption. Although the exact temperature of this process is unknown, it is supposed to be higher than 300 K. Thus, the final selection of conformers should be done in the FES rather than on the PES. Table 2 contains the relative free Gibbs energies and relative populations obtained from the RR-HO-IG (RI-MP2/cc-pVDZ) calculations on the 10 most stable conformers according to the relative enthalpies energy scale (see Table 1). Assuming a Boltzmann distribution at 300 K, six conformers (wg01, wg08, wg02, wg07, wg03 and wg09; see Figure 2) are more likely to be populated at the experimental conditions. Boltzmann distributions calculated at even higher temperatures (data not shown) predict the same conformers to be among the most populated ones. The REMPI spectrum of Trp-Gly dipeptide shows the presence of at least four different conformers[10,11] although the exact number of isomers coexisting in the gas phase could be higher. Surprisingly, the first, third, and fifth most populated conformers are not being observed experimentally (see the discussion below about the assignment of the spectra). Although the consideration of RR-HO-IG approximation could bring some uncertainty to our calculations and, consequently, the relative order of the conformers could be slightly changed, the relative proportions of conformer populations in the thermodynamic equilibrium should be reliable. Thus, two questions arises: (a) why is the most populated conformer (the global minimum conformation) not observed experimentally? and (b) why are the third and fifth structures having relative populations very similar to the fourth and sixth conformers not observed? We suggest the following explanations. The signal of one of the conformers observed in the REMPI spectrum was too weak to obtain IR−UV hole-burning spectra with sufficient noise. This signal could correspond to the global minimum conformation and then, this could be the reason this conformer was not experimentally observed. Broad absorptions were observed in the REMPI spectrum. Broad absorptions have been theoretically explained in case of DNA bases in terms of a pathway for rapid internal conversion,[32,33] in other words, if excited states have very short lifetimes. The same situation could also be happening in the case of the Trp-Gly dipeptide, thus preventing the detection of some of the theoretically predicted conformers. Finally, since at the beginning of the experiment the sample is cooled in a supersonic jet, the absence of some conformers could also be associated to collisional relaxation of these conformers to the most stable ones through low-energy barriers.[34] It seems then quite probable that some information cannot yet be obtained from the spectroscopic measurements. In this respect, the theoretical studies nicely complement the experiments, and they can be very useful for unravelling future REMPI and hole-burning spectra of similar peptides.

Table 3 contains the scaled theoretical IR frequencies for the six most populated conformers ($T = 300$K) of Trp-Gly dipeptide. The experimental frequencies are also included. The mid (3100−3600 and 1100−1800 cm^{-1}) theoretical and experimental IR ground state spectra are schematically shown in Figure 3. The 3100−3600 cm^{-1} spectral region shows three lines of absorption corresponding to the carboxyl O−H stretching (OH), the indole N−H stretching (NH_{ind}) and the peptide N−H stretching (NH_{pep}) vibrations. The four bands observed in the 1100−1800 cm^{-1} spectral region can be assigned to the carbonyl of carboxyl group and carbonyl peptide stretching vibrations (CO_{carb} and CO_{pep}, respectively), the peptide N−H

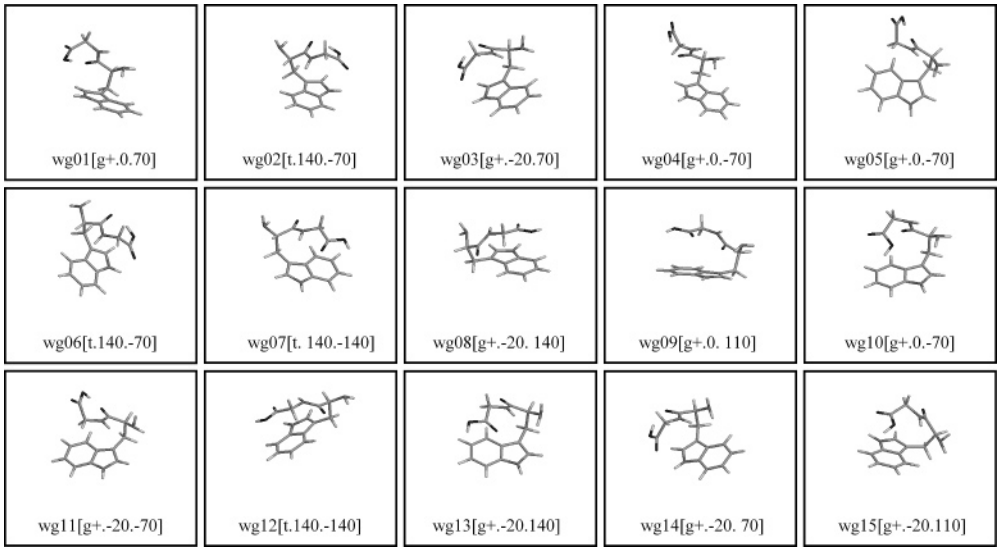

Figure 1. RI-MP2/cc-pVTZ geometries for the 15 most stable structures of Trp-Gly dipeptide.

CHART 3: (a) Trp Amino Acid, Trp-Gly and Trp-Gly-Gly Sequence of Peptides. (b) Overlap of the Peptide Backbone of the Most Stable Conformers in the PES of Trp-Gly-Gly and Phe-Gly-Gly Tripeptides

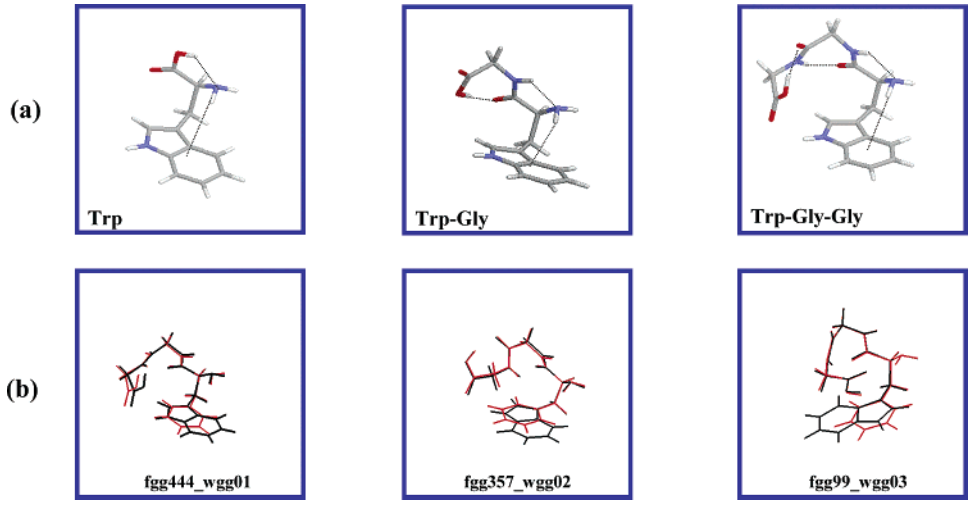

in-plane bending vibration (NH_{ipb}) and to the carboxyl O−H in-plane bending vibration (OH_{ipb}).

From the analysis of the scaled theoretical IR spectra two families of conformers can be easily distinguished: (a) those for which the OH and OH_{ipb} absorption bands correspond to the free (not hydrogen bonded) O−H stretching vibration of the carboxyl group in a syn configuration (wg08, wg07, and wg09) and (b) those for which the OH and the OH_{ipb} bending modes are shifted (about 300 cm^{-1} to a lower and higher frequency, respectively) with respect to the unperturbed stretch, thus suggesting the involvement of the OH in an intramolecular H-bond (wg01, wg03, and wg02). Surprisingly, no experimental evidence has been reported by Kleinermanns and co-workers on the existence of conformers with an $OH_{carb}\cdots O{=}C_{pep}$ intramolecular H-bond. Instead, a stretched, unfolded structure where the NH_{pep} bond is possibly involved in an intramolecular interaction is suggested.[11] Interestingly, three of the six most populated conformers (wg08, wg07, and wg09) show the suggested geometrical feature (see Figure 2), and consequently their theoretical IR spectra have been compared with the experimental ones.

wg08, wg07, and wg09 IR spectra mainly differ in the NH_{pep} stretching vibration frequency (νNH_{pep}) (see Table 3 and Figure 3). The same discrepancy is observed in case of the experimental spectra (**a**, **b**, and **d**). This large sensitivity of νNH_{pep} to conformational changes provides the key to assign **a**, **b**, and **d** spectra to a single conformer. On one hand, in wg08, νNH_{pep} is significantly red-shifted (free νNH_{pep} in *N*-acetyl tryptophan methyl amide (NATMA) ranges between 3454 and 3466 cm^{-1} depending on the conformer[35]) as the NH_{pep} bond is involved in two H-bond interactions: $NH_{pep}\cdots N(H_2)$ and $NH_{pep}\cdots\pi$ (see Figure 2). Conformer **d** also shows a significantly red-shifted νNH_{pep}. Notice, however, that for conformer **d** no signal was measured in the 1100−1800 cm^{-1} spectral region, and thus, no sufficient experimental data are available for a proper comparison. In the case of wg07, the NH_{pep} bond only benefits from a $NH_{pep}\cdots\pi$ intramolecular H-bond (see Figure 2), and νNH_{pep} is only slightly red-shifted. NH_{pep} absorption line of conformer **b** appears at a similar frequency than that of wg07 (see Table 3). Finally, wg09 conformer shows a νNH_{pep} closer to an unperturbed NH_{pep} bond. In wg09 (see Figure 2), the NH_{pep} bond is neither clearly oriented to the lone pairs of the nitrogen of the amino group nor close enough to the aromatic rings. Therefore, its involvement in either a $NH_{pep}\cdots N(H_2)$ or $NH_{pep}\cdots\pi$ intramolecular H-bond is smaller than in case of wg08 or wg07 conformers. Conformer **a** also shows a νNH_{pep} very close to the unperturbed one**.** From the previous analysis, the experimental spectrum **a** could be assigned to conformer wg09,

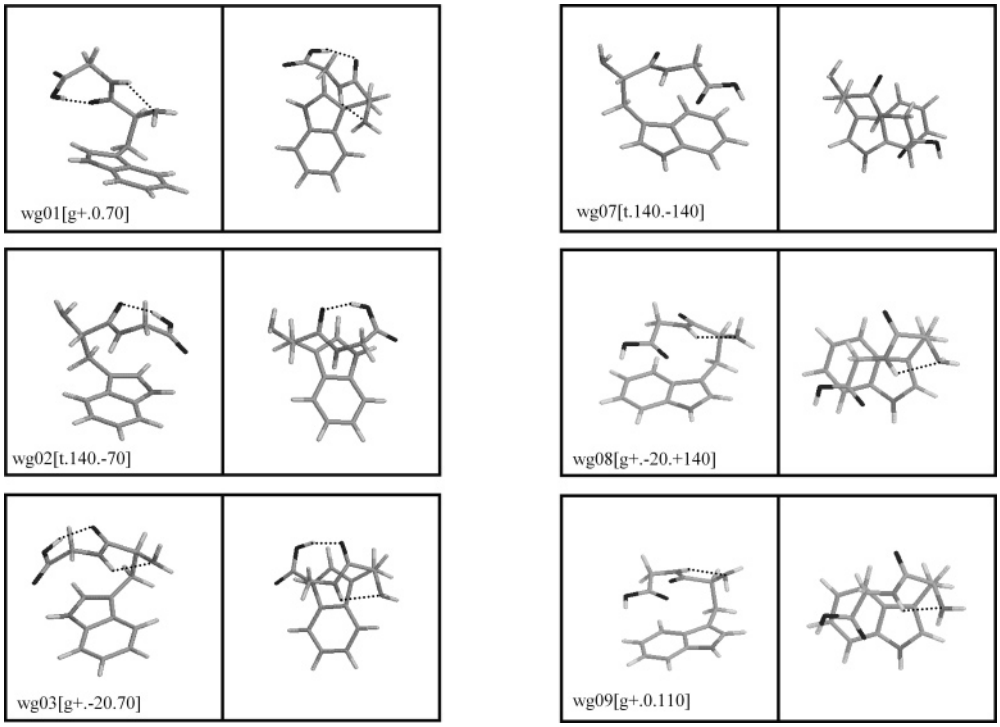

Figure 2. Six most populated structures in the FES of Trp-Gly dipeptide. The OH is involved in an intramolecular H-bond for all of the structures in the left column.

TABLE 3: Experimental (a, b, and d) and Calculated Vibrational Frequencies (cm^{-1}) for the Six Most Populated Conformers in the FES of Trp-Gly Dipeptide

conformer	OH^a	$NH_{ind}{}^b$	$NH_{pep}{}^c$	$CO_{carb}{}^a$	$CO_{pep}{}^a$	$NH_{ipb}{}^a$	$OH_{ipb}{}^a$
wg01[g+.0.70]	3177	3518	3396	1776	1659	1512	1430
wg03[g+.−20.70]	3193	3502	3407	1763	1664	1511	1421
wg02[t.140.−70]	3252	3498	3414	1762	1653	1503	1409
d	**3598**	**3522**	**3407**				
wg08[g+.−20.140]	3599	3528	3391	1760	1706	1485	1133
b	**3582**	**3522**	**3412**	**1789**	**1705**	**1516**	**1106**
wg07[t.140.−140]	3598	3528	3416	1758	1695	1480	1142
a	**3588**	**3519**	**3422**	**1794**	**1705**	**1502**	**1129**
wg09[g+.0.110]	3594	3527	3432	1762	1701	1496	1131

[a] The scaling factor for the OH frequency and for all the mid-IR bands was set at 0.956. [b] The scaling factor for NH_{ind} frequency was set at 0.958. [c] The scaling factor for NH_{pep} frequency was set at 0.951.

b to conformer wg07 and finally **d**, to conformer wg08. Besides, for wg09 and wg07 structures, the 1100−1800 cm^{-1} spectral region shows trends (see Table 3) parallel to those of conformers **a** and **b**, respectively, thus reinforcing the suggested assignment of the spectra (the 1100−1800 cm^{-1} spectral region of conformer **d** could not be measured). However, wg09 and wg07 spectra are so similar we cannot fully disregard the possibility that wg09 could be assigned to conformer **b** and wg07 to conformer **a**. Finally, it should also be noticed that the calculated frequencies nicely agree with those measured experimentally.

When comparing the spectra of Trp-Gly dipeptide conformers with those of the Trp amino acid conformers,[4] some interesting similarities can be found. Trp spectra can also be grouped in two families according to their OH and OH_{ipb} bending modes. As for the dipeptide, these bending modes are significantly shifted when the OH is involved in a $OH\cdots N(H_2)$ intramolecular H-bond. The remaining absorption lines appear at the same frequency values as their analogues in the Trp-Gly dipeptide.

Trp-Gly-Gly. Table 4 contains information similar to that collected in Table 1 for the 13 most stable minima localized in the PES of Trp-Gly-Gly tripeptide. It should be noticed that, as in the case of Trp-Gly dipeptide, we selected the 15 most stable minima at the RIMP2/cc-pVTZ//RIMP2/cc-pVDZ level of theory (see Chart 1) for an ab initio RI-MP2/cc-pVTZ optimization. However, two structures converged to two already existing minima, and thus, they were not considered for the final ab initio treatment. The CCSD(T) energy correction term accounts for up to 1.81 kcal/mol, and therefore, its inclusion is decisive for determining the final relative energies as well as for obtaining the proper order of structures. Notice that at the RI-MP2 level of theory (columns 2−4 in Table 4), the global minimum, as well as the first, second, third, fifth, eleventh, and twelfth local minima, remain in the same order but at the CBS/CCSD(T) level of theory (column 6) the relative position of most of the conformers (even that of the global minimum) changes. The CCSD(T)/CBS procedure substantially increases the relative energies, and now, the 13 structures presented in Table 4 lie within an interval of energy of about 4.5 kcal/mol. Unlike for the Trp-Gly and Phe-Gly-Gly[1] peptides, in the case of the Trp-Gly-Gly tripeptide, the inclusion of the ZPE corrections (see column 7) changes the order of stabilities of the conformers with respect to that stated according to the electronic energies (column 6). Besides, for the Trp-Gly-Gly tripeptide only four structures lie within 2 kcal/mol relative enthalpy limit, whereas for the other peptides, 10 structures were present in the same energetic range.

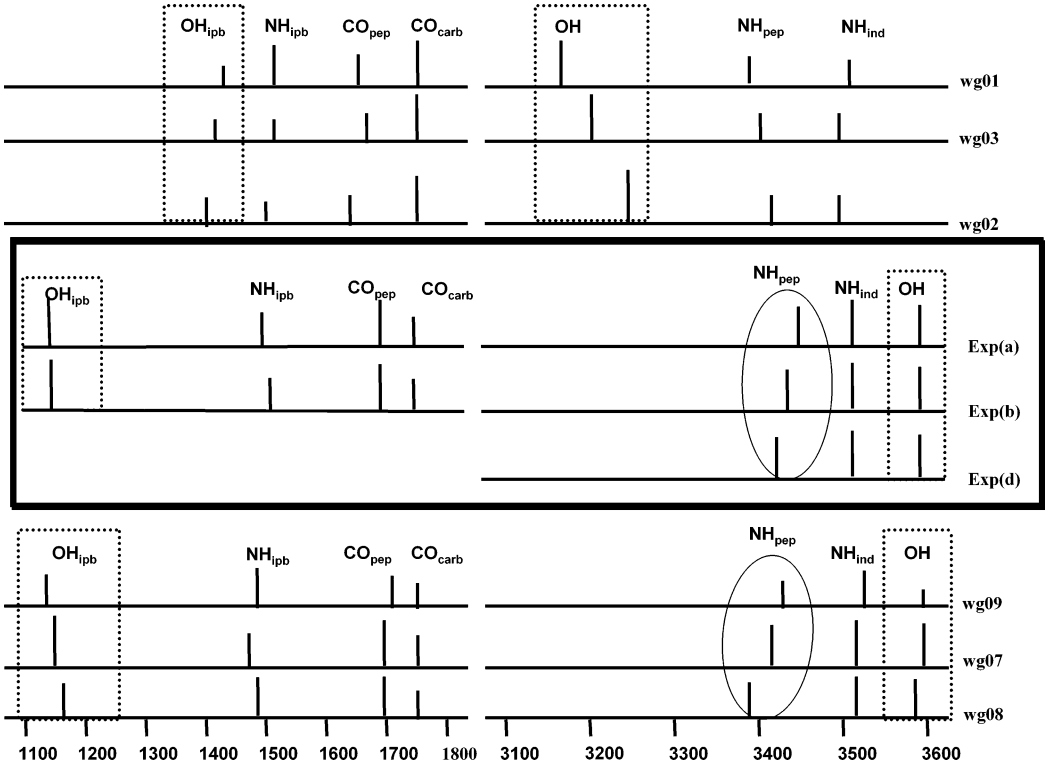

Figure 3. Schematic diagrams of the experimental and theoretical (RIMP2/cc-pVDZ) harmonic (scaled) spectra of the Trp-Gly dipeptide.

TABLE 4: Relative Energies and Relative Enthalpies at 0 K (in kcal/mol) for the Most Stable Conformers of Trp-Gly-Gly Tripeptide Evaluated with Various Basis Sets (Structures Are Labeled According to Figure 4)

structure	RI-MP2/cc-pVTZ	RI-MP2/cc-pVQZ	T → Q[a]	MP2 → CCSD(T)[b]	*E*[c]	*H*[d]
wgg01[g+.0.70.−60.−70]	0.16	0.34	0.47	−0.47	0.00	0.00
wgg02[g+.0.110.0.70]	0.00	0.00	0.00	0.42	0.42	0.10
wgg03[g+.20.70.−60.−70]	1.55	1.56	1.57	0.75	2.32	1.76
wgg04[t.140.−70.60.70]	1.93	2.13	2.28	−0.03	2.24	1.99
wgg05[g+.20.70.−60.−70]	2.09	2.09	2.09	0.19	2.27	2.03
wgg06[t.140.−100.0.−70]	3.05	2.84	2.68	0.38	3.06	2.44
wgg07[g+.−20.70.−60.−70]	1.86	2.35	2.70	0.05	2.75	2.53
wgg08[g+.−20.140.−110.−70]	0.99	1.29	1.51	1.34	2.85	2.66
wgg09[t.140.−70.60.70]	2.84	3.01	3.14	−0.09	3.05	2.79
wgg10[t.−20.70.−60.−70]	3.50	3.59	3.66	−0.28	3.38	2.99
wgg11[g+.0.110.0.70]	3.19	3.11	3.04	1.00	4.04	3.16
wgg12[g+.−20.140.−110.−70]	2.61	2.78	2.90	1.29	4.19	4.10
wgg13[t.140.−140.110.70]	3.48	3.54	3.58	0.97	4.55	4.25

[a] Extrapolation to the CBS limit using cc-pVTZ and cc-pVQZ energies. [b] Difference between CCSD(T) and MP2 relative energies determined with the 6-31g*(0.25) basis set. [c] Total relative energy evaluated as a sum of CBS RI-MP2 relative energy and a difference between CCSD(T) and MP2 relative energies. [d] ZPE were calculated at the RIMP2/cc-pVDZ level of theory.

RIMP2/cc-pVTZ geometries for the 13 most stable conformers in the PES of the Trp-Gly-Gly tripeptide are depicted in Figure 4. For all of the minima, both peptide bonds are in a *trans* conformation. The first conformer in the PES in which one of the two peptide bonds is in a *cis* conformation is ∼8.5 kcal/mol higher in energy (at the RI-MP2/cc-pVTZ//RI-MP2/cc-pVDZ level of theory as for this structure the CBS extrapolation was not calculated) than the global minimum. All of the minima collected are either in a g+ or in a *trans* rotameric state. The first conformer in a g− rotameric state is 7.8 kcal/mol less stable (RIMP2/cc-pVTZ). The global minimum, wgg01, adopts the conformation with the maximum number of H-bonds (see Figure 5): $OH_{carb}\cdots C{=}O_{pep}$, $C{=}O_{pep}\cdots HN_{pep}$, $C{=}O_{carb}\cdots HN_{ind}$ and $NH_{pep}\cdots N(H_2)\cdots\pi$ cooperative H-bond. The first local minimum, wgg02, is only 0.1 kcal/mol less stable than the global minimum (see column 7 in Table 4). Both structures essentially differ in the orientation of the second glycyl residue (see Figure 5). More specifically, in wgg02, the ψ_2 angle differs ∼60° from its analogue in wgg01, and consequently, the $C{=}O_{pep}\cdots HN_{pep}$ intramolecular interaction is not formed. Unless for this intramolecular interaction, the H-bond pattern of both structures is the same, so it is tempting to explain the lower stability of wgg02 in terms of the absence of the $C{=}O_{pep}\cdots HN_{pep}$ H-bond interaction. wgg03, corresponding to one of the experimentally observed structures (see discussion about the assignment of the spectra below), shows a different H-bond pattern than wgg01 and wgg02. The $C{=}O_{pep}\cdots HN_{pep}$ and $NH_{pep}\cdots N(H_2)$ H-bond interactions remain but now, no $OH_{carb}\cdots C{=}O_{pep}$, $C{=}O_{carb}\cdots HN_{ind}$ and $NH_{pep}\cdots\pi$ intramolecular H-bonds are formed. Instead, the carbonyl of the carboxyl group is interacting with one of the hydrogen atoms of the amino group.

The H-bond pattern of Trp-Gly-Gly tripeptide is obviously far more complex than that of the dipeptide and the amino acid. For the tripeptide, the peptide backbone is longer and clearly, there is a larger number of possible H-bond donor/acceptor binding sites. Specifically, three more intramolecular H-bonds

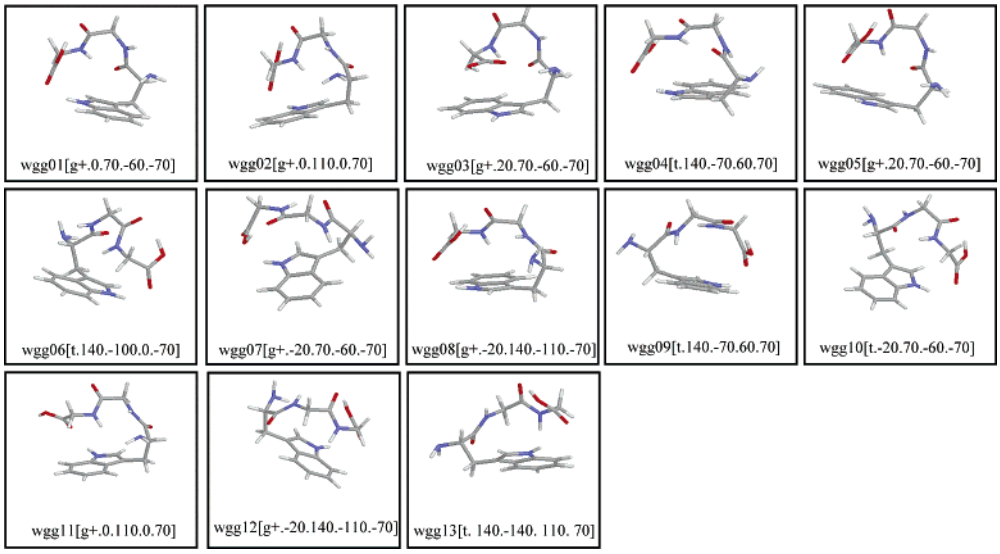

Figure 4. RI-MP2/cc-pVTZ geometries for the 13 most stable structures of Trp-Gly-Gly tripeptide.

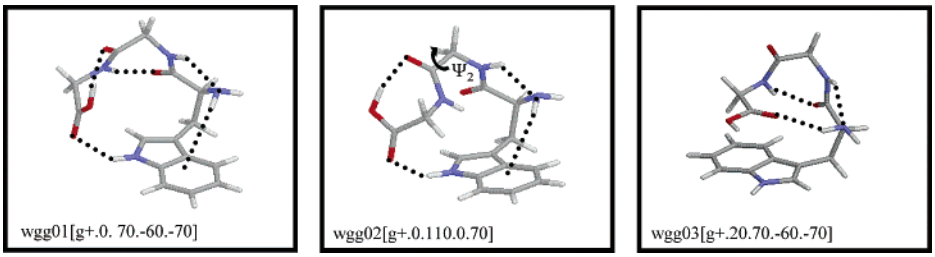

Figure 5. Three most stable structures in the FES of Trp-Gly-Gly tripeptide.

can be formed: $C{=}O_{pep}\cdots HN_{pep}$, $C{=}O_{carb}\cdots HN_{ind}$, and $C{=}O_{carb}\cdots H_2N$. However, few geometrical similarities can still be found between Trp-Gly-Gly and Trp and Trp-Gly global minimum conformations (see Chart 3a). First, the peptide backbone is folded. Second, g+ rotameric states are systematically preferred. Third, the carboxyl group is in an anti configuration. And fourth, a $NH_{pep}\cdots N(H_2)\cdots\pi$ ($OH\cdots N(H_2)\cdots\pi$ in case of Trp amino acid) cooperative hydrogen bonded "daisy chain" interaction is present. Obviously, there is a systematic geometric behavior in the sequence Trp amino acid, Trp-Gly dipeptide and Trp-Gly-Gly tripeptide. Besides, two families of conformers can be distinguished for each system, depending whether the carboxyl group is involved in intramolecular H-bond or not.

The three most stable conformers of the PES of Trp-Gly-Gly have also been compared with those three most stable conformers on the PES of the Phe-Gly-Gly[1] tripeptide (see Chart 3b). Specifically, the overlap of the peptide backbones of the different peptides was studied. As can be seen from Chart 3b, the geometries of the peptide backbones are essentially the same. Moreover, the orientation of the side chains is also equivalent. Thus, a systematic structural behavior is observed for the tripeptides containing two glycyl residues, and therefore, it is expected that the most stable conformers of other similar peptides would present equivalent geometries.

Statistical thermodynamic calculations are essential to understand the relative abundance of conformers at thermodynamic equilibrium. Thus, relative free Gibbs energies and populations assuming a Boltzmann distribution at $T = 300$ K were calculated for the 13 most stable minima on the PES of Trp-Gly-Gly (see Table 5). From a detailed inspection of Table 5, it can be seen that passing to the free Gibbs energies, significantly changes the relative stabilities of the conformers in comparison to the

TABLE 5: Relative Free Gibbs Energies (*G*) and Corresponding Relative Populations Calculated at $T = 300$ K According to the Maxwell−Boltzmann Distribution (MBD) Equation for the 13 Most Stable Conformers of Trp-Gly-Gly Tripeptide

structure	*G* (kcal/mol)	MBD
wgg02[g+.0.110.0.70]	0.00	1000
wgg01[g+.0.70.−60.−70]	0.51	427
wgg11[g+.0.110.0.70]	1.90	41
wgg03[g+.20.70.−60.−70]	1.91	40
wgg07[g+.−20.70.−60.−70]	2.19	25
wgg05[g+.20.70.−60.−70]	2.30	21
wgg04[t.140.−70.60.70]	2.50	15
wgg08[g+.−20.140.−110.−70]	2.84	8
wgg06[t.140.−100.0.−70]	2.91	7
wgg09[t.140.−70.60.70]	3.43	3
wgg10[t.−20.70.−60.−70]	3.46	3
wgg12[g+.−20.140.−110.−70]	5.07	0
wgg13[t.140.−140.110.70]	5.20	0

CBS/CCSD(T) results (see column 6 of Table 4). The first local minimum (wgg02) at the CBS/CCSD(T) level of theory becomes now the global minimum and vice versa. The second (wgg03) and third (wgg04) local minima in the PES are the third and sixth local minima in the FES. Besides, the relative position of the remaining conformers also changes, and wgg11 (tenth local minima according to the enthalpies scale) is now the third most stable conformer in the free Gibbs energies scale. Our statistical thermodynamic calculations show that wgg02 as well as wgg01 are highly populated. Apart from these two abundant conformers, there is a set of conformers with very small but equal population. According to the REMPI experiments on Trp-Gly-Gly tripeptide two conformers (**a** and **b**) were observed to coexist in the gas phase. In addition, the existence of a third structure was also suggested. The experimentally observed structures correspond to the first (wgg02) and fourth

TABLE 6: Experimental (a and b) and Calculated Vibrational Frequencies (cm^{-1}) for the Most Populated Conformers of Trp-Gly-Gly

conformer	OH^a	$NH_{ind}{}^b$	$NH_{pep1}{}^c$	$NH_{pep2}{}^c$	$CO_{carb}{}^a$	$CO_{pep1}{}^a$	$CO_{pep2}{}^a$	$NH_{ipb2}{}^a$	$NH_{ipb1}{}^a$	$OH_{ipb}{}^a$
a		**3381**	**3419**	**3431**	**1771**	**1671**^{d}	**(????)**^{d}	**1551**	**1504**	**1421**
wgg02[g+.0.110.0.70]	3208	3352	3411	3431	1746	1709	1662	1510	1477	1420
b	**3585**	**3520**	**3396**	**3388**	**1782**	**1716**	**1681**	**1510**^{d}	**(????)**^{d}	**1106**
wgg03[g+.20.70.−60.−70]	3600	3524	3408	3394	1761	1715	1679	1498^d	(1480)^d	1110
wgg01[g+.0.70.−60.−70]	3129	3424	3393	3270	1749	1678^d	(1660)^d	1534	1493	1420
wgg04[t.140.−70.60.70]	3140	3469	3417	3301	1756	(1656)^d	167^d	1531	1503	1425
wgg05[g+.20.70.−60.−70]	3221	3497	3412	3388	1757	1688	1659	1513	1487	1416
wgg06[t.140.−100.0.−70]	3248	3372	3482	3411	1749	1706	1664	1508	1747	1413
wgg07[g+.−20.70.−60.−70]	3139	3455	3421	3267	1754	(1660)^d	1681^d	1536	1506	1426
wgg08[g+.−20.140.−110.−70]	3152	3473	3399	3395	1753	1706	1650	1517	1487	1424
wgg09[t.140.−70.60.70]	3139	3465	3435	3297	1756	1679	1660	1532	1511	1425
wgg10[t.−20.70.−60.−70]	3149	3421	3426	3264	1750	1688	1661	1538	1491	1430
wgg11[g+.0.110.0.70]	3591	3409	3414	3461	1752	1708^d	(1706)^d	1498	1468	1152
wgg12[g+.−20.140.−110.−70]	3161	3477	3482	3382	1756	1696	1645	1518	1477	1424
wgg13[t.140.−140.110.70]	3166	3474	3479	3390	1754	1702	1649	1519	1496	1423

[a] The scaling factor for the OH frequency and all the mid-IR bands was set at 0.956. [b] The scaling factor for NH_{ind} frequency was set at 0.958. [c] The scaling factor for NH_{pep} frequency was set at 0.951. [d] Neighboring vibration modes are coupled, the band with the value in parentheses has marginal intensities; (????) means that experimental value of coupled vibration mode with marginal intensity could not be measured.

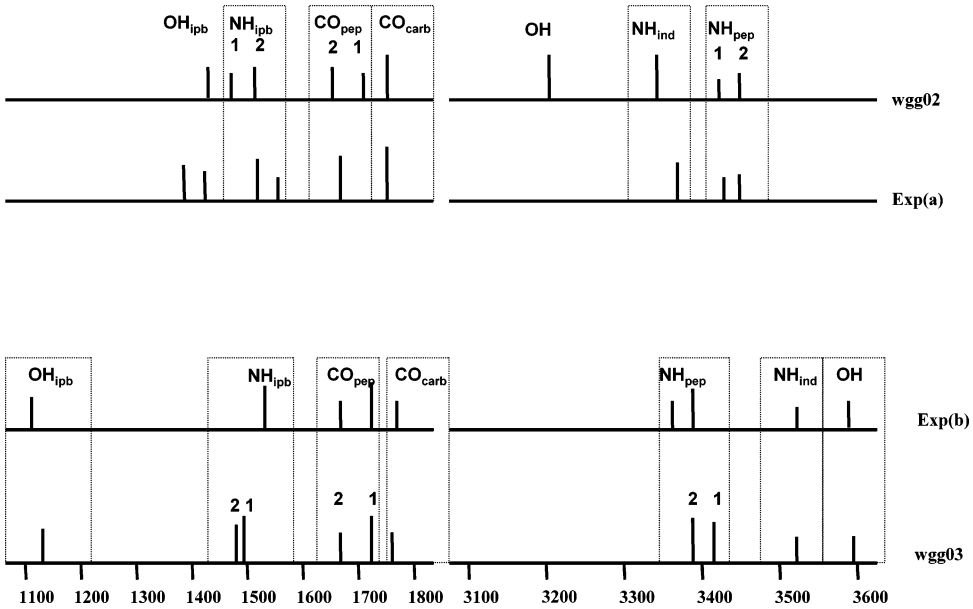

Figure 6. Schematic diagrams of the experimental and theoretical (RIMP2/cc-pVDZ) harmonic (scaled) spectra of Trp-Gly-Gly tripeptide. Numbers 1 and 2 stand for the absorption lines of both peptide bonds.

(wgg03) most stable conformers according to the free Gibbs energy scale (see the discussion about assignment of the spectra below). Surprisingly, neither the second most populated structure (wgg01) nor conformers with similar population as conformer **b** (wgg11) were experimentally detected. As has been already discussed for the Trp-Gly dipeptide, the calculated abundances of conformers should be representative of the relative proportions of structures observed at thermodynamic equilibrium. The question that now arises is as follows: how is it possible that no experimental evidence is obtained about conformers of similar stabilities and abundances than those already observed. The difficulty for obtaining high-resolution spectra and thus, conclusive experimental results, can be one of the reasons. However, it should also be taken into account that a collisional relaxation of conformers may occur during the free jet expansion.[36] Another possible explanation could be given in terms of the lifetime of the excited conformers. If it is very short, they may decay very fast to the ground state and thus, the two-photon spectroscopy becomes less efficient, preventing the detection of some of these conformers.

The RIMP2/cc-pVDZ frequencies of the 13 most stable minima of Trp-Gly-Gly were compared to those experimentally measured. Table 6 contains the scaled theoretical and experimental IR frequencies for these structures. Figure 6 displays schematically the spectra for the experimentally observed structures and the corresponding calculated ones. The 3100−3600 cm^{-1} spectral region shows four lines of absorption corresponding to the carboxyl O−H stretching vibration (OH), the indole N−H stretching (NH_{ind}) and the peptide N−H stretching vibrations of the two peptide bonds (NH_{pep1} and NH_{pep2}). The 1100−1800 cm^{-1} spectral region contains six absorption lines that can be assigned to the carbonyl of carboxyl group and carbonyl peptide stretching vibrations (CO_{carb}, CO_{pep1}, and CO_{pep2}), two peptide N−H in-plane bending vibrations (NH_{ipb1} and NH_{ipb2}) and to the carboxyl O−H in-plane bending vibration (OH_{ipb}). Conformers **a** and **b** can be clearly assigned to conformers wgg02 and wgg03, respectively, as the scaled theoretical IR spectra of these structures match the experimental ones (see Figure 6). Notice, however, that since the experimental IR spectrum of conformer **a** was measured in the range from

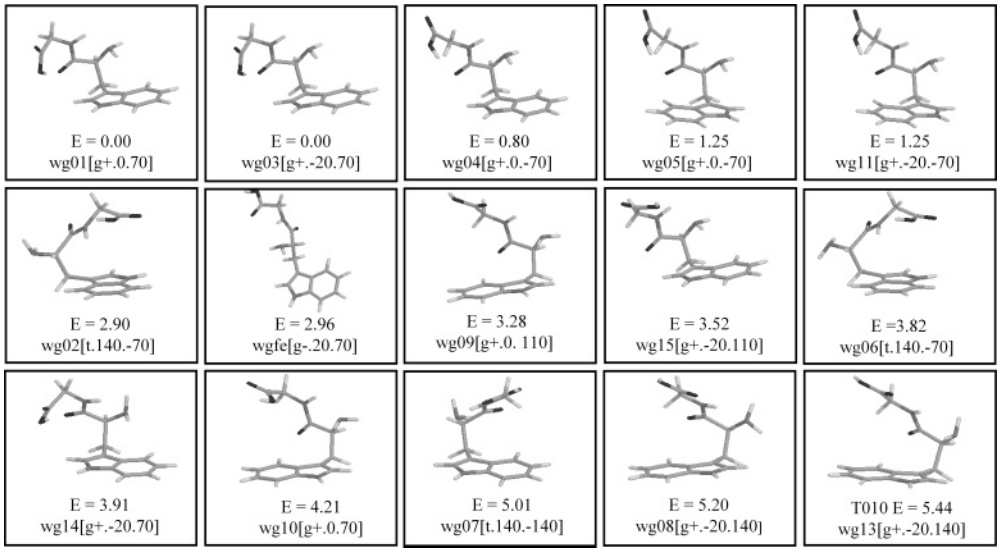

Figure 7. RI-TPSS/cc-pVTZ geometries and relative energies for the 15 most stable conformers of Trp-Gly dipeptide. wgfe is the most stable structure in a $g-$ rotameric state.

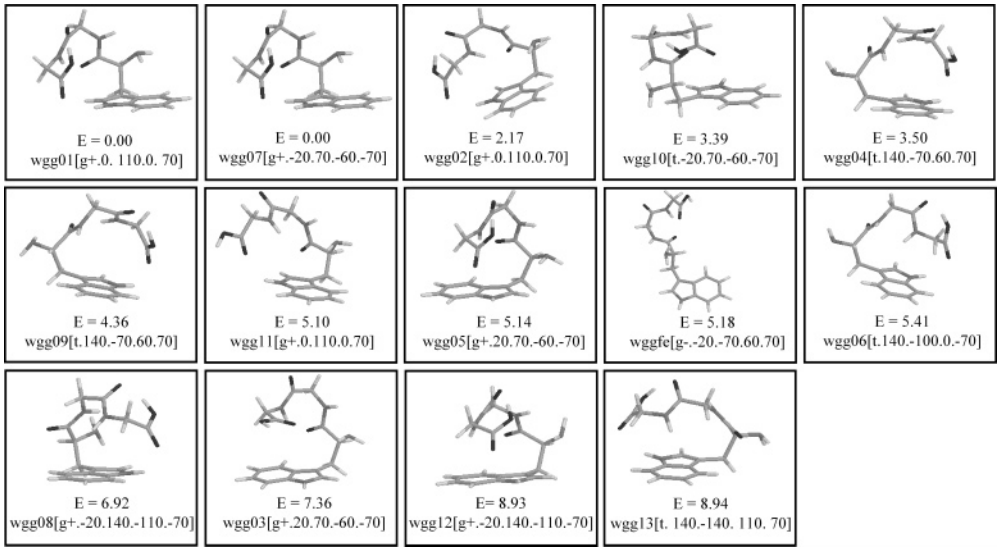

Figure 8. RI-TPSS/cc-pVTZ geometries and relative energies for the 13 most stable conformers of Trp-Gly-Gly tripeptide. wggfe is the most stable structure in a $g-$ rotameric state.

3250 cm^{-1} up to 3600 cm^{-1}, the red-shifted OH stretch band with a frequency value around 3200 cm^{-1} was not experimentally detected. Besides, two more absorption lines were detected (at 1393 and 1421 cm^{-1}), although experimentalists[11] were not able to determine which of them belongs to OH_{ipb} stretching vibration. In case of conformer **b**, only one absorption line was observed for NH_{ipb} as the other one was strongly coupled and so close to the first one, that it was impossible to distinguish them. Undoubtedly, the second and third most populated conformers, wgg01 and wgg11 (see Table 5), cannot be assigned to any of those experimentally observed conformers (see Table 6).

Evaluation of the Performance of the DFT Methodology. The performance of the DFT methodology has been evaluated for the Trp-Gly and Trp-Gly-Gly peptides. RI-MP2/cc-pVTZ-optimized structures (see Figures 1 and 4) have been used as a trial set. Final relative energies of the di- and tripeptide (column six of Tables 1 and 4) calculated as a sum of CBS RI-MP2 relative energies and a CCSD(T) correction term have been chosen as the benchmark data. RI-TPSS/cc-pVTZ-optimized geometries and relative energies are presented in Figures7 and 8 for the Trp-Gly and Trp-Gly-Gly, respectively. The nomenclature of the conformers refers to the RI-MP2/cc-pVTZ geometries used as the initial structures for the DFT optimization. The RI-DFT global minima of the two peptides agree with the ones predicted at the RI-MP2 level. However, conformers which are local minima according to the benchmark energies (the second local minimum of Trp-Gly and the sixth local minimum of Trp-Gly-Gly) converged to the global minimum at the RI-DFT level of theory. Besides, the order of conformers according to the DFT scale strongly differs from the RI-MP2 one. Regarding RI-DFT geometries, notice that, unless for the global minima, they are significantly different to the RI-MP2 ones, especially for those conformers where the peptide backbone is bent over the aromatic side chain. More specifically, conformers where the glycyl residue lies over the aromatic ring (i.e., wg05 in Figure 1) or where the carbonyl of the carboxyl group interacts with the indole ring (i.e., wg03 in Figure 1) are not reproduced at the DFT level. It is clear then, that the overlap between the peptide backbone and the aromatic side chain is not well described at the DFT level and thus, DFT theory does not provide the proper geometries of some of the conformers.

As is well-known from the literature,[37] DFT theory does not properly cover the London dispersion energy, and thus, fails to describe those conformers where, the dispersion energy is playing a relevant role in their stabilization. Subsequently, DFT theory should be used with extreme care when studying aromatic amino acids and small aromatic peptide systems.[38]

A final remark should be done concerning the DFT structures suggested by Kleinermanns and co-workers for the observed conformers.[10,11] From the REMPI and UV−UV and IR−UV hole-burning experiments on the Trp-Gly dipeptide and Trp-Gly-Gly tripeptide no information concerning the geometry of the systems could be obtained. Therefore, experiments were combined with DFT calculations performed on a set of structures designed by chemical intuition. In any of the cases, it was possible to make a clear assignment of the conformers. Besides, none of the structures suggested by Kleinermanns and co-workers, resembles the most stable conformers according to the RI-MP2 predictions. For the sake of comparison, Kleinermanns and co-workers proposed structures were calculated at the RI-MP2 level of theory. All of them are less stable than the conformers here suggested.

Conclusions

(i) The combination of ab initio SCC-DFTB-D MD/Q simulations with high-level correlated ab initio quantum chemical calculations has proven to be an efficient tool for obtaining a complete conformational landscape of amino acids and small peptide systems.

(ii) Structures and relative energies of the lowest energy conformers were determined on the basis of complete basis set limit RI-MP2 energy and a CCSD(T)/6-31G*(0.25) correction term (evaluated for the RI-MP2/cc-pVTZ-optimized geometries).

(iii) Common geometrical features have been systematically observed for the sequence Trp, Trp-Gly, and Trp-Gly-Gly. Geometrical similarities have also been found when the comparison was made with other aromatic peptide systems.

(iv) Statistical thermodynamic calculations are essential for the understanding of the relative populations of conformers at conditions of thermodynamic equilibrium. Passing from the analysis of the PES to the FES is necessary since the order of stability of the structures differ on these surfaces significantly. Statistical thermodynamic calculations nicely complement the experimental results and provide information about those peptides where obtaining well resolved spectra is not possible.

(v) Scaled theoretical IR frequencies agree well with the experimental ones. Unlike for the DFT calculations, the comparison of the calculated ab initio spectra with the measured ones allows for an unambiguous assignment of the conformers.

(vi) DFT methodology fails to describe the stabilization resulting from the London dispersion energy. Some of the conformers gain stability from the London dispersion interaction between the peptide backbone and the aromatic side chain and these conformers are at the DFT level wrongly characterized. The use of DFT for the study of small peptides containing aromatic rings cannot be thus recommended.

Acknowledgment. This work has been part of the research project Z4 055 905 and was supported by grants from the grant agency of the Academy of Sciences of the Czech Republic (Grant No. A400550510), Ministry of Education of the Czech Republic (Center for Biomolecules and Complex Molecular Systems, LC512), and National Science Foundation under Contract No. CHE-0244341. H.V. holds the EMBO scholarship (Grant No. ALTF 580-2003). We thank Jiří Vondrášek and Martin Kabeláč for their interesting comments and suggestions. We also acknowledge Prof. Karl Kleinermann's collaboration concerning the DFT calculations. Tomas Schultz nicely helped us with the understanding of the experimental technique.

References and Notes

(1) Řeha, D.; Valdés, H.; Vondrášek, J.; Hobza, P.; Abu-Riziq, A.; Crews, B.; de Vries, M. S. *Chem. Eur. J.* **2005**, *11*, 6803−6817.

(2) Řeha, D.; Kabeláč, M.; Ryjáček, F.; Šponer, J.; Šponer, J. E.; Elstner, M.; Suhai, S.; Hobza, P. *J. Am. Chem. Soc.* **2002**, *124*, 3366−3376.

(3) Snoek, L. C.; Robertson, E. G.; Kroemer, R. T.; Simons, J. P. *Chem. Phys. Lett.* **2000**, *321*, 49−56.

(4) Robertson, E. G.; Simons, J. P. *Phys. Chem. Chem. Phys.* **2001**, *3*, 1−1819.

(5) Grace, L. I.; Cohen, R.; Dunn, T. M.; Lubman, D. M.; de Vries, M. S. *J. Mol. Spectrosc.* **2002**, *215*, 204−219.

(6) Kovacevic, B.; Rozman, M.; Klasinc, L.; Srzic, D.; Maksic Z. B.; Yanez, M *J. Phys. Chem. A.* **2005**, *109*, 8329−8335.

(7) Cohen, R.; Brauer, B.; Nir, E.; Grace, L. de Vries, M. S. *J. Phys. Chem. A* **2000**, *104*, 6351−6355.

(8) Kapota, C.; Ohanessian, G. *Phys. Chem. Chem. Phys.* **2005**, *7*, 3744−3755.

(9) Cable, J. R.; Tubergen, M. J.; Levy, D. H. *J. Am. Chem. Soc.* **1988**, *110*, 7349−7355.

(10) Hunig, I.; Kleinermanns, K *Phys. Chem. Chem. Phys.* **2004**, *6*, 2650−2658.

(11) Bakker, J. M.; Plützer, C.; Hünig, I.; Häber, T.; Compagnon, I.; von Helden, G.; Meijer, G.; Kleinermanns, K. *Chem. Phys. Chem.* **2005**, *6*, 120−128.

(12) Brauer, B.; Gerber, R.; Kabelac, M.; Hobza, P.; Bakker, J. M.; Abu-Riziq, A.; de Vries, M. S. *J. Chem. Phys. A* **2005**, *109*, 6974−6984.

(13) Elstner, M.; Hobza, P.; Frauenheim, T.; Suhai, S.; Kaxiras, E. *J. Chem. Phys.* **2001**, *114*, 5149−5155.

(14) Elstner, M.; Frauenheim, T.; Kaxiras, E.; Seifert, G.; Suhai, S. *Phys. Status Solidi B−Basic Res.* **2000**, *217*, 357−376.

(15) Ryjáček, F.; Engkwist, O.; Vacek, J.; Kratochvíl, M.; Hobza, P. *J. Phys. Chem. A* **2001**, *105*, 1197−1202.

(16) Feyereisen, M.; Fitzgerald, G.; Komornicki, A. *Chem. Phys. Lett.* **1993**, *208*, 359−363.

(17) Vahtras, O.; Almlöf, J.; Feyereisen, M. W. *Chem. Phys. Lett.* **1993**, *213*, 514−518.

(18) Bernholdt, D. E.; Harrison, R. J. *Chem. Phys. Lett.* **1996**, *250*, 477−484.

(19) Dunning, T. H., Jr. *J. Chem. Phys.* **1989**, *90*, 1007−1023.

(20) Kendall, R. A.; Dunning, T. H., Jr. *J. Chem. Phys.* **1992**, *96*, 6796−6806.

(21) Halkier, A.; Helgaker, T.; Jørgensen, P.; Klopper, W.; Koch, H.; Olsen, J.; Wilson, A. K. *Chem. Phys. Lett.* **1998**, *286*, 243−252.

(22) Jurečka, P.; Hobza, P. *Chem. Phys. Lett.* **2002**, *365*, 89−94.

(23) Hobza, P.; Šponer, J. *J. Am. Chem. Soc.* **2002**, *124*, 11802.

(24) Dąbkowska, I.; Valdés-González, H.; Jurečka, P.; Hobza, P. *J. Phys. Chem. A* **2005**, *109*, 1131−1136.

(25) Tao, J.; Perdew, J. P.; Staroverov, V. N.; Scuseria, G. E. *Phys. Rev. Lett.* **2003**, *91*, 146401.

(26) Becke, A. D. *Phys. Rev. A* **1988**, *38*, 3098−3100.

(27) Ahlrichs, R.; Bär, M.; Häser, M.; Horn, H.; Kölmel C. *Chem. Phys. Lett.* **1989**, 162, 165−169.

(28) MOLPRO, a package of ab initio programs designed by H.-J. Werner and P. J. Knowles, version 2002.1. Amos, R. D.; Bernhardsson, A.; Berning A.; Celani, P.; Cooper, D. L.; Deegan, M. J. O.; Dobbyn, A. J.; Eckert, F.; Hampel, C.; Hetzer, G.; Knowles, P. J.; Korona, T.; Lindh, R.; Lloyd, A. W.; McNicholas, S. J.; Manby, F. R.; Meyer, W.; Mura, M. E.; Nicklass, A.; Palmieri, P.; Pitzer, R.; Rauhut, G.; Schütz, M.; Schumann, U.; Stoll, H.; Stone, A. J.; Tarroni, R.;; Thorsteinsson, T.; Werner. H.-J. University College Cardiff Consultants, Ltd.: Cardiff, 2002.

(29) Frisch, M. J.; Trucks, G. W.; Schlegel, H. B.; Scuseria, G. E.; Robb, M. A.; Cheeseman, J. R.; Montgomery, J. A., Jr.; Vreven, T.; Kudin, K. N.; Burant, J. C.; Millam, J. M.; Iyengar, S. S.; Tomasi, J.; Barone, V.; Mennucci, B.; Cossi, M.; Scalmani, G.; Rega, N.; Petersson, G. A.; Nakatsuji, H.; Hada, M.; Ehara, M.; Toyota, K.; Fukuda, R.; Hasegawa, J.; Ishida, M.; Nakajima, T.; Honda, Y.; Kitao, O.; Nakai, H.; Klene, M.; Li, X.; Knox, J. E.; Hratchian, H. P.; Cross, J. B.; Bakken, V.; Adamo, C.; Jaramillo, J.; Gomperts, R.; Stratmann, R. E.; Yazyev, O.; Austin, A. J.; Cammi, R.; Pomelli, C.; Ochterski, J. W.; Ayala, P. Y.; Morokuma, K.; Voth, G. A.; Salvador, P.; Dannenberg, J. J.; Zakrzewski, V. G.; Dapprich, S.; Daniels, A. D.; Strain, M. C.; Farkas, O.; Malick, D. K.; Rabuck, A. D.; Raghavachari, K.; Foresman, J. B.; Ortiz, J. V.; Cui, Q.; Baboul, A. G.; Clifford, S.; Cioslowski, J.; Stefanov, B. B.; Liu, G.; Liashenko, A.;

Piskorz, P.; Komaromi, I.; Martin, R. L.; Fox, D. J.; Keith, T.; Al-Laham, M. A.; Peng, C. Y.; Nanayakkara, A.; Challacombe, M.; Gill, P. M. W.; Johnson, B.; Chen, W.; Wong, M. W.; Gonzalez, C.; Pople, J. A. *Gaussian 03*, revision C.02; Gaussian, Inc.: Wallingford, CT, 2004.

(30) Chocholoušová, J.; Špirko, V.; Hobza, P. *Phys. Chem. Chem. Phys.* **2004**, *6*, 37−41.

(31) Poulain, P.; Antoine, R.; Broyer, M.; Dugourd, P. *Chem. Phys. Lett.* **2005**, *401*, 1−3.

(32) Abo-Riziq, A.; Grace, L.; Nir, E.; Kabeláč, M.; Hobza, P.; de Vries, M. S. *Proc. Natl. Acad. Sci. U.S.A.* **2005**, *102*, 20−23.

(33) Sobolewski, A. L.; Domcke W. *Phys. Chem. Chem. Phys.* **2004**, *6*, 2763−2771.

(34) Leasrri, A.; Cocinero, E. J.; Lopez, J. C.; Alonso, J. L. *Chem. Phys. Chem.* **2005**, *6*, 1559−1566.

(35) Dian, B. C.; Longarte, A.; Zwier, T. S. *J. Chem. Phys.* **2003**, *118*, 2696−2706.

(36) Godfrey, P. D.; Brown, R. D. *J. Am. Chem. Soc.* **1998**, *120*, 10724−10732.

(37) Hobza, P.; Šponer, J. *J. Chem. Rev.* **1999**, *99*, 3247−3276.

(38) Vondrášek, J.; Bendová, L.; Klusák, V.; Hobza, P. *J. Am. Chem. Soc.* **2005**, *127*, 2615−2619.